PFC/RR-85-25 DOE/ET-51013-167

SAFETY AND PROTECTION FOR LARGE SCALE SUPERCONDUCTING MAGNETS - FY1985 REPORT

by

R.J. Thome, J.V. Minervini, R.D. Pillsbury, Jr.
H.D. Becker, W.R. Mann

December 1985

Submitted to Idaho National Engineering Laboratory
Idaho Falls, Idaho

Table of Contents

List of Figures

List of Tables

1.0 Introduction

The magnetic field intensities required in a fusion reactor are tens of thousands of times stronger than those which occur naturally and they must be produced in relatively large volume containers. The magnetic fields are generated by complex coil systems which, together with their power supplies and control subsystems, represent some of the largest and most sophisticated electrical equipment built to date. The forces which are developed within the magnets are so high that the structural requirements often dominate other engineering considerations in the design process. As a result, the magnet systems, which are the backbone of the device for confinement and control of the plasma, are a formidable engineering challenge.

MIT has been carrying out a program for INEL oriented toward safety and protection in large scale magnet systems. The program involves collection and analysis of information on actual magnet failures, analysis of general problems associated with safety and protection, and performance of safety oriented experiments. This report summarizes work performed under this program in FY 1985.

This year a collaboration has been established with Kernforschungszentrum (KfK), Karlsruhe, FRG. MIT has a staff engineer (M.M. Steeves) at KfK for a six month assignment with the TESPE Team, which is directed by Dr. K.P. Jüngst. TESPE is a facility composed of six superconducting "D-shaped" coils mounted on a common circle to simulate the toroidal field coils in a tokamak. The facility has been operated up to its design field level of 7 T and will now be used in a series of tests specifically oriented toward safety and protection issues. The facility and recent tests are outlined in Section 2.0. MIT expects to support the on-site activity at KfK with analytical effort and code development at MIT. These tests are expected to be a significant contribution to the understanding of safety and protection issues relative to superconducting magnet system operation. At present, for example, a test sequence involving a short circuit across one of the coils is being planned.

Section 3.0 presents a summary of a magnet safety and accident survey which was performed by MIT in support of MESA Corporation with DOE funding. A survey format was constructed to request information on the system description, subsystem in which the failure initiated, failure sequence initiator, and failure event. Tables were constructed and data reduced for a total of 31 events. In summary, there were no loss of life or personnel injury incidents, but significant schedule alterations were required in 19 cases. In 12 of the 19 cases, the event was such that no change in operating scenario was required when modifications were complete, but in 7 cases physical and economic constraints were such that operation with an altered scenario was necessary.

In past reports we considered the problem of magnetic to kinetic energy conversion in a magnet system following a structural failure. This is an area of continuing interest and since the determination of the stored energy is the first step in any analysis of this type, Section 4.0 presents a collection of formulae and graphs which allow the estimation of the inductance or stored energy for toroidal field coils. Results were collected or derived for several cross-sectional shapes of interest, namely: circular, elliptical, "Princeton-D," and rectangular.

Section 5.0 describes the failure experience with two different pulse coils used to provide a time varying field for experiments with internally cooled cabled conductors. The failure modes were analyzed and found to be consistent with straightforward observations and computations. In one case, the failure occurred due to creep in the copper turns of the inner pulse coil which is subject to substantial tensile loading during operation. The second failure involved buckling of the outer layer of conductor under the action of the inward radial pressure experienced during operation. Solutions to these specific problems for these coils are outlined.

Section 6.0 describes other safety-related activities under this program. This involved further analysis for the ORNL LCTF activity to study possible means for removal of another short circuit in the instrumentation within the GE LCP coil. This is a continuation of a similar activity under this program in 1983 in which analyses were performed by MIT

and ORNL and a short discovered at that time was subsequently removed. A second area in this category of activity was the use of some of the previous work under this program by an MIT grad student as one of the case studies for sophomore engineers to illustrate potential problem areas in design.

The fusion program is building and operating the largest magnet systems in the world. A thorough understanding of the possible failure modes and the means for their prevention is essential. This program continues to contribute to this area through small scale tests and analysis of actual magnet failures. It has now expanded to an international collaborative activity as a means for leveraging the available resources.

2.0 Collaboration with Kernforschungszentrum, Karlsruhe, FRG

2.1 Description of TESPE

The TESPE facility[1] at KfK was built specifically to investigate toroidal field coil system fabrication and operational characteristics. It consists of a set of six, D-shaped superconducting coils mounted on a common circle in typical tokamak toroidal field (TF) coil fashion. The system has been tested in a three coil[2] and six coil[3] mode up to its design field level and is presently being used in a magnet-safety-oriented test program. The overall characteristics of the system are outlined in the following table.

Table 2.1

Major Characteristics of TESPE

Torus Overall OD	2.55 m
Major Radius	0.81 m
Minor Radius at Midplane	0.26 m
Bore Elongation	0.62 m
Operating Current	7 kA
Maximum Field	7 T
Stored Energy	8.8 MJ
Overall Current Density	7×10^7 A/m^2
Copper Current Density	3×10^8 A/m^2
Cu/NbTi	1.8:1
Mass of Six Coils	4200 kg
Mass of Intercoil Structure	2900 kg
Total Cold Mass	8000 kg

Each of the coils is wound with a composite conductor of copper and NbTi superconductor. The coils are bath-cooled with liquid helium with each coil in a separate helium vessel. The helium vessels are fed from a common reservoir with the reservoir and all

helium vessels in a single room temperature vacuum chamber.

The general scale and shape of one of the coils and of the system are indicated in Figures 2.1 and 2.2, respectively. These illustrate current filament models which have been constructed by MIT for use in supporting calculations for the TESPE program as part of the collaboration next year.

2.2 Range of Collaboration

MIT presently has a staff engineer (M.M. Steeves) on site at KfK as part of this collaborative effort. He will participate in the TESPE testing program and in tests on a small coil system supplied by MIT as part of the poloidal field coil development program. The latter coil developed a short circuit during the fabrication process and is currently being analyzed as part of this safety and protection program (results will be reported next year).

Tests to date on TESPE have focused on achieving design values[2,3] and testing coil stability[3]. Other tests are underway to investigate the buckling characteristics associated with the unstable equilibrium position of one TF coil between the adjacent coils. These tests are being done as part of a thesis project (W. Geiger, KfK).

In the recent buckling tests, the centering force on each coil was taken only at the bucking post and buckling loads between adjacent TF coils were determined as a function of current level by setting the current, applying an impulse load and measuring the natural frequencies of the system. At low current levels, the measured frequencies are low and imply a buckling load corresponding to currents near the design operating level; however, at higher current levels, gaps close, the structure stiffens, the natural frequencies increase, and the implied buckling loads are well above the design current level. These tests are expected to continue over the near term.

Tests have also begun on the investigation of the impact of a vacuum leak in the main vessel. This was begun by cooling down the system, then breaking the main vacuum

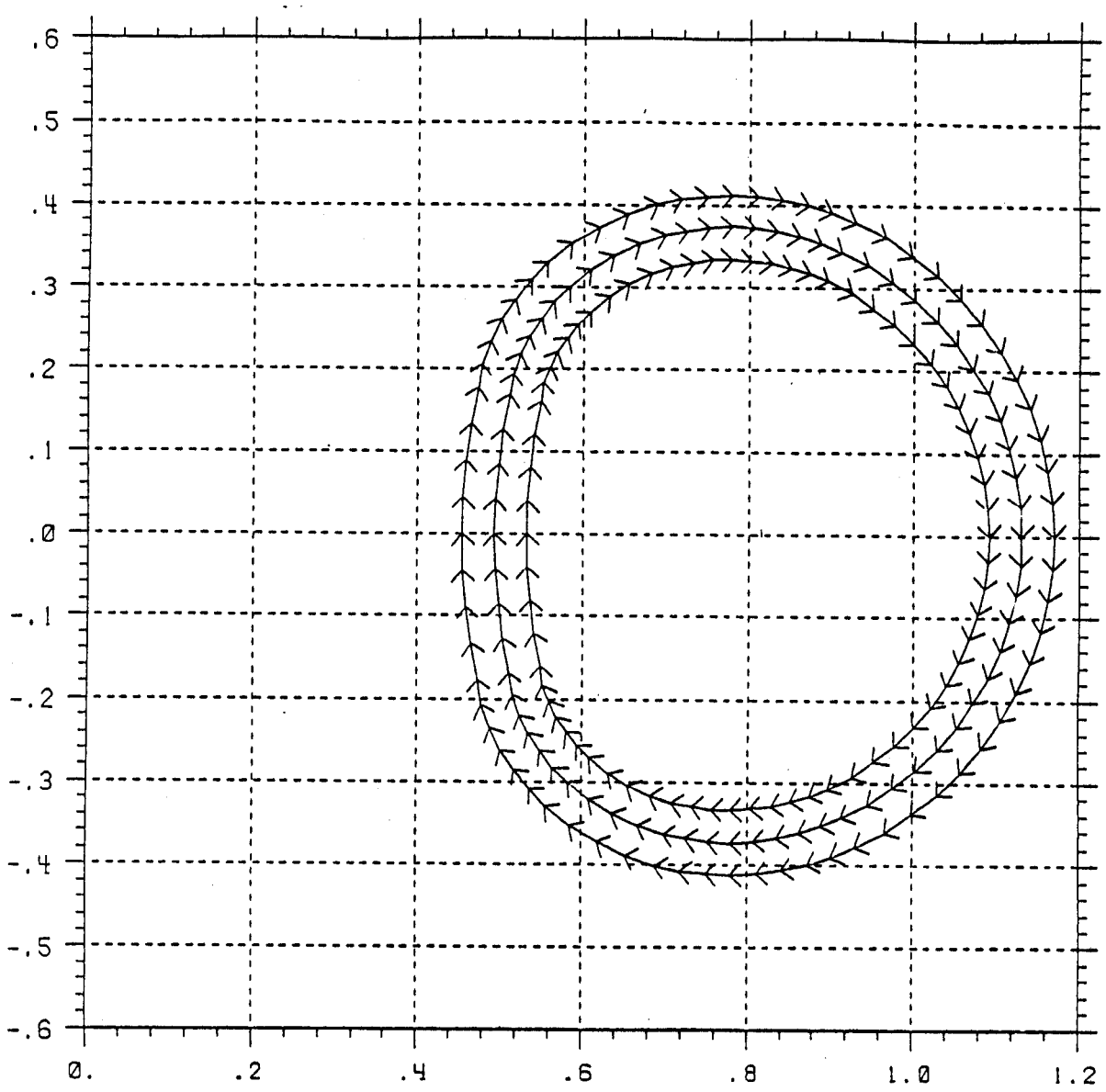

Fig. 2.1 Elevation View of Current Stick Model of One TESPE TF Coil

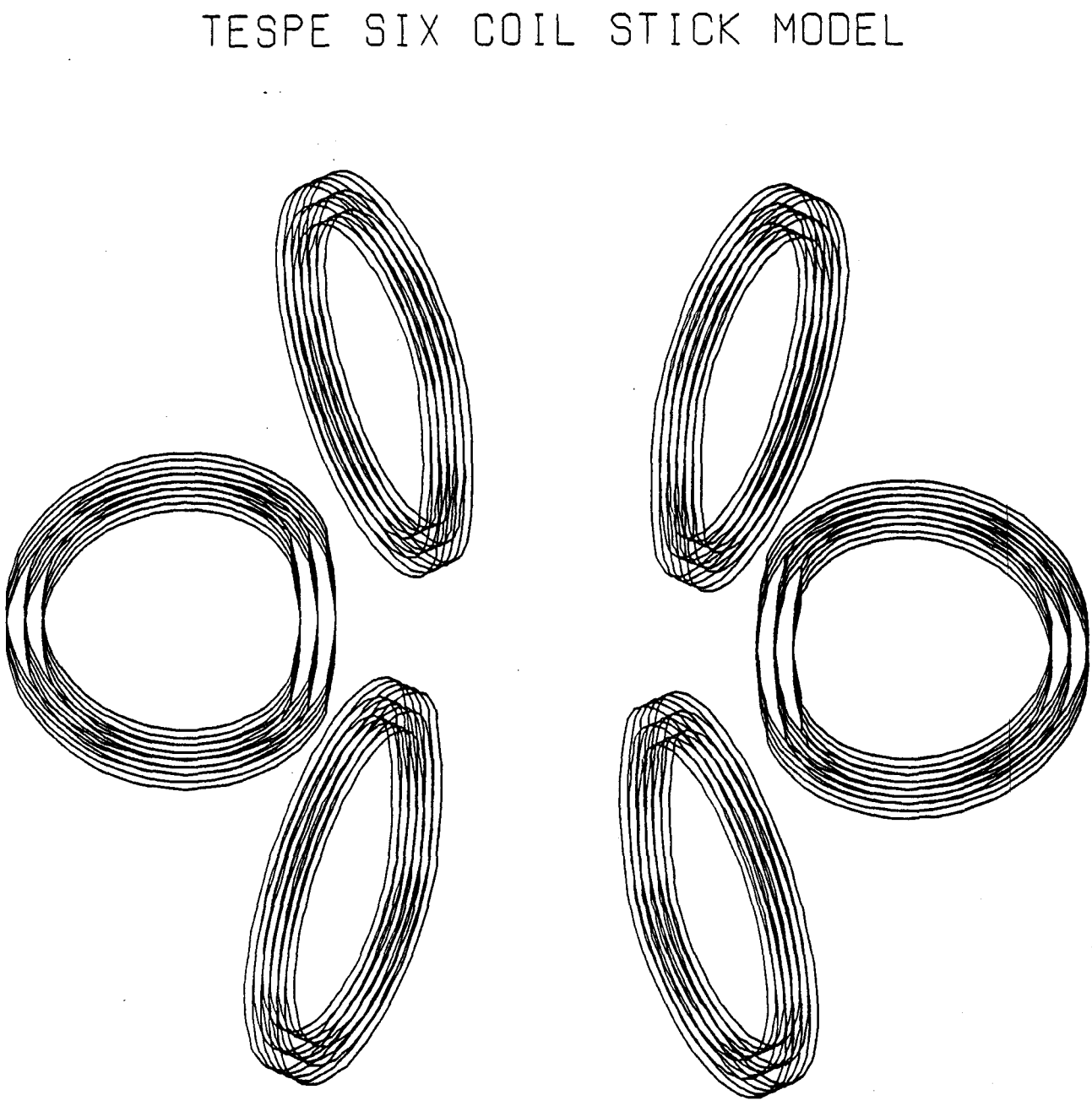

Fig. 2.2 Current Stick Model of Six Coil TESPE Torus

with a small, known mass of helium gas. Data involving the change in the boil-off rate of cryogens from the liquid helium vessels and from the liquid-nitrogen-cooled shield were taken and are being analyzed at KfK.

The next series of tests will involve operational characteristics of the system with a short circuit across one of the TF coils. A resistor is currently under construction at KfK and plans are under development for a test sequence currently scheduled for January, 1986.

Based on a data package transmitted to KfK, they have determined that the "football" test module[4] at MIT would be geometrically compatible with TESPE and is of potential interest because it is wound with an internally cooled, cabled conductor (ICCS). They are also considering the bath-cooled modules[4] available at MIT. We will determine the facility and module modifications required relative to cost and test data benefits to evaluate whether this tack should be pursued.

MIT is planning to support the activity analytically, and is presently building a computer model of the system to estimate lumped parameter characteristics for use in calculations involving the short circuit test program.

———— References for Section 2.0

[1] K.P. Jüngst and TESPE Team, "Status Report of TESPE," IEEE Trans. Magnetics, vol MAG-17, no. 5, Sept., 1981.

[2] K.P. Jüngst and L. Yan, "Stability of the TESPE Superconducting Torus Magnets," Appld. Superconductivity Conference, San Diego, Sept., 1984.

[3] K.P. Jüngst, G. Friesinger, and W. Geiger, "Superconducting Torus TESPE at Design Values," Inter. Conf. on Magnet Technology (MT-9), Zurich, Sept., 1985.

[4] R.J. Thome, "The Football Experiment–Simulation of ICCS Operation in a Large Scale Magnet," 1980 Superconducting MHD Magnet Design Conf, MIT, March, 1980.

3.0 Magnet Safety and Accident Survey

This program provided some support to MIT in an effort with MESA Corporation to perform a survey of magnet-related accidents in the USA. Results are contained in a separate report [1], but the introduction to the report has been modified and reproduced in this section because it is a good summary of the survey and is of general interest in large magnet safety and protection.

The goal was to survey the major centers of magnet design and operation in the United States to obtain information on magnet system accident and failure events, then summarize and classify the events. The purpose is to educate future designers relative to actual experience with problem areas which can have an impact on magnet system safety, reliability, and availability.

A survey format was constructed which requested summary information on the system description, subsystem in which the failure initiated (where), failure sequence initiator (why), and failure event (how). This involved a set of four tables together with definitions of entry labels. Sample entries were obtained by direct contact with two laboratories, then the survey and samples were mailed to a list of 20 DOE National Laboratories and DOD Laboratories in the United States. Responses were obtained and further discussions held with 18 sources which led to data on 31 individual events. A glossary of terms in the survey tables and the tabular responses are contained in the main report [1] together with a short description of each event.

The tabulated responses are extensive in that they were intended to allow entries for a large range of system applications and different levels of system complexity. This section summarizes the information by accumulating the responses on four simplified tables. Although there is some danger in over-simplification, there are some trends indicated. In reviewing this material, it is necessary to bear in mind that most, if not all, of these systems are one-of-a-kind systems which were often designed to push the state-of-the-art in one or more technical areas.

In each of the 31 cases, the respondent was asked to rank the criticality of the event. Table 3.1 lists the criticality level definitions and gives the total responses in the survey for each level. Note that there were no loss-of-life or personnel injury (Level 1) events and that events are distributed toward the lower criticality levels. However, significant project schedule alterations were required in 19 cases. In 12 of the 19 cases, the event was such that no change in operating scenario was required when modifications were complete, but in 7 cases physical or economic constraints were such that operation with an altered scenario was necessary. We should also recognize that there are probably a large number of events which are in category five, but which were considered too insignificant to report.

TABLE 3.1

SUMMARY OF EVENT CRITICALITY

CRITICALITY LEVEL	DEFINITION	NO. OF EVENTS
1	Loss of life or personnel injury	0
2	System damaged beyond repair feasibility (i.e., physical and economic)	1
3	System damage sufficient for significant project schedule slip and requires altered (reduced rating) scenario	7
4	System damage sufficient for significant project schedule slip and requires no change in operating scenario	13
5	System damage resulted in little or no schedule slip and no change in operating scenario	9
		30 EVENTS = TOTAL

In the survey, respondents were asked to judge the cause of the failure based on the list in Table 3.2 and to consider whether the listed cause was a primary or contributing factor. Results were necessarily subjective in nature and the total number of times each cause was indicated in the survey is given in the table. Bear in mind that all events are not equal in criticality and systems vary drastically in size and complexity. The responses indicated that inadequate design, assembly, and operation, in that order, were the primary failure causes. This is to be expected from the one-of-a-kind, advanced technological character of these devices, but also implies a lack of experience or quality assurance. Note that one case involved the intentional test of the system to failure.

A list of items for how failures could be initiated was prepared and the total response in each category is summarized in Table 3.3. In this table the total is greater than 31 because of the large uncertainty in responses concerning primary vs contributing factors. Hence, each entry is the total number of times an item was listed as either a primary or contributing factor. The bulk of the failures were initiated by arcing and sparking or by mechanical overload which is consistent with the generally high electromagnetic loading and high power or stored energy associated with these devices. It is also interesting to note that false signals and responding to false signals was identified as an important area.

The systems in the survey spanned a wide range of size and complexity. Respondents were asked to identify the subsystem in which the failure was initiated and to identify subsystems into which the failure propagated. The sums of the responses for each subsystem are given in Table 3.4 which must be considered in view of the fact that most of the systems contain only a small number of the items in the list. Nevertheless, the table implies that the majority of the problems were initiated in coil windings. A review of the more extensive tables and event descriptions in the main report [1] implies inadequately applied insulation or the electrical or mechanical overload of insulation as important factors. The overload was often attributed to inadequate or optimistic design and sometimes to improper operation.

The intent of this survey was to gather information on actual failure experience from

the designers and facility operators who are breaking ground on the forefront of magnet system technology and applications. We are indebted to them for their time and candor and hope that the experiences which they have outlined can guide future designers in concentrating their efforts in those areas which have been the primary failure sources of the past. In this way, the lessons of experience will contribute to the improvement of reliability and availability in future systems.

TABLE 3.2

SUMMARY OF FAILURE SEQUENCE INITIATORS (i.e., - "why") IN 31 EVENTS

CAUSE	PRIMARY FACTOR	CONTRIBUTING FACTOR
Improper Assembly*	8	2
Improper Operation	5	2
Inadequate SOP	3	5
Design Error	13	7
Unbecoming Acts	0	0
Natural Events	0	0
Insufficient QC	1	8
Intentional Failure Test	1	0
	31 EVENTS	

* e.g. - Improper assembly was a primary factor in initiating a failure event in 8 cases and was a contributing factor in 2 cases.

TABLE 3.3

SUMMARY OF FAILURE EVENT CATEGORIES (i.e. - "how") IN 31 EVENTS

ITEM	PRIMARY OR CONTRIBUTING FACTOR
Local Fire	0
Electric Power Loss	0
Loss of Utilities	0
Missiles	0
Inundation by Water	0
Thermal Cycling Fatigue*	2
Mechanical Cycling Fatigue	4
Mechanical Abrasion	2
Defective Materials	3
Adulteration of Chemicals or Phase Change	3
Arcing and Sparking	10
False Signals	5
Mechanical Overload	8
Other	5

* e.g. - Thermal Cycling Fatigue was either a primary or contributing factor in 2 cases.

TABLE 3.4

SUMMARY OF INITIAL FAILURE LOCATIONS(i.e. - "where") FOR 31 EVENTS

Subsystem	Failure Source	Effected by Failure in source
GHe Storage	0	0
Compressor	0	0
Cold Box	0	0
LHe Dewar*	1	1
LHe Control System	0	0
Purifier	0	0
Vacuum System	1	0
LN_2 Storage and Supply	0	2
LN_2 Control System	0	1
LHe Vessel	0	1
Radiation Shield	0	1
Vacuum Tank	0	1
Gravity Supports	2	0
Vapor-cooled Leads	4	2
Coil Winding	11	5
Coil Structure	3	1
Water Pumps	0	0
Water Heat exchangers	0	0
Water Supply	0	0
Magnet Power Supply	0	2
Bus Work	0	2
Dump Circuits	3	0
Instrumentation and Control	6	0
Bldg. Services	0	0
	31 Events	

* e.g. - The LHe dewar was the source of failure in one event and was affected by the source of failure in one event.

Reference for Section 3.0

[1] J.B. Czirr and R.J. Thome, "Experience with Magnetic Accidents-Phase III Report," MESA Corp, March 7, 1985.

4.0 Magnetic to Kinetic Energy Conversion

4.1 Background Information

In previous studies [1,2] we have shown that a magnet failure which is potentially catastrophic in the sense that structural components fracture and the winding suffers extensive plastic deformation can be "safe" under special conditions. It may be desirable to limit operating current densities to levels at which the winding could act to inhibit magnetic to kinetic energy conversion. The conclusions from a simplified model showed that:

a) A protective circuit reaction involving resistive dissipation following a major structural failure is unlikely to be effective on a fast enough time scale in high current density windings.

b) Windings with low enough current densities can absorb the total load following structural failure, thus limiting the energy conversion process, although this may involve substantial yielding and deformation of the winding.

c) Protective circuits involving inductive energy transfer can respond fast enough to limit the energy conversion process in high or low current density systems and are effective provided they are well coupled to the primary circuit and the latter is able to carry the loads which result.

The primary quantity of interest to this type of problem is the magnetic energy stored in the system. In a tokamak, the toroidal field (TF) coil system tends to operate at the highest field and has the most complex geometry and structure. In the following section we have collected and derived closed-form expressions for the inductance for several TF coil geometries to allow easy estimation of stored energies.

4.2 Inductance (Stored Energy) Estimation for TF Systems

This section summarizes simple closed form expressions and graphs for estimating the inductance and, in turn, the energy for TF coil systems with selected geometries. In all cases, a very thin winding is assumed. This tends to underestimate the energy because it neglects the energy stored within the winding itself; however, for preliminary estimation purposes, the results are adequate. Four thin-shell axisymmetric cases are treated with the following cross sections: circular, elliptical, "Princeton-D," and rectangular.

Figure 4.1 shows the normalized inductance for a thin shell, circular-cross-section torus as a function of aspect ratio. The expression for this case is given by:

$$\frac{L}{\mu_0 N^2 a} = \frac{R}{a}\left[1 - \sqrt{1 - (R/a)^{-2}}\right] \tag{4.1a}$$

where: N = total number of turns in torus winding.

The expression for the elliptical cross-section system can be reduced to a similar form and found from the same figure by using

$$\frac{L}{\mu_0 N^2 b} = \frac{a}{b}\left(\frac{L}{\mu_0 N^2 a}\right) \tag{4.1b}$$

where a and b are now the radii of the principal axes of the ellipse as indicated in Fig. 4.1.

The "Princeton-D" cross section is a constant tension shape where the tension parameter, k, is given by:

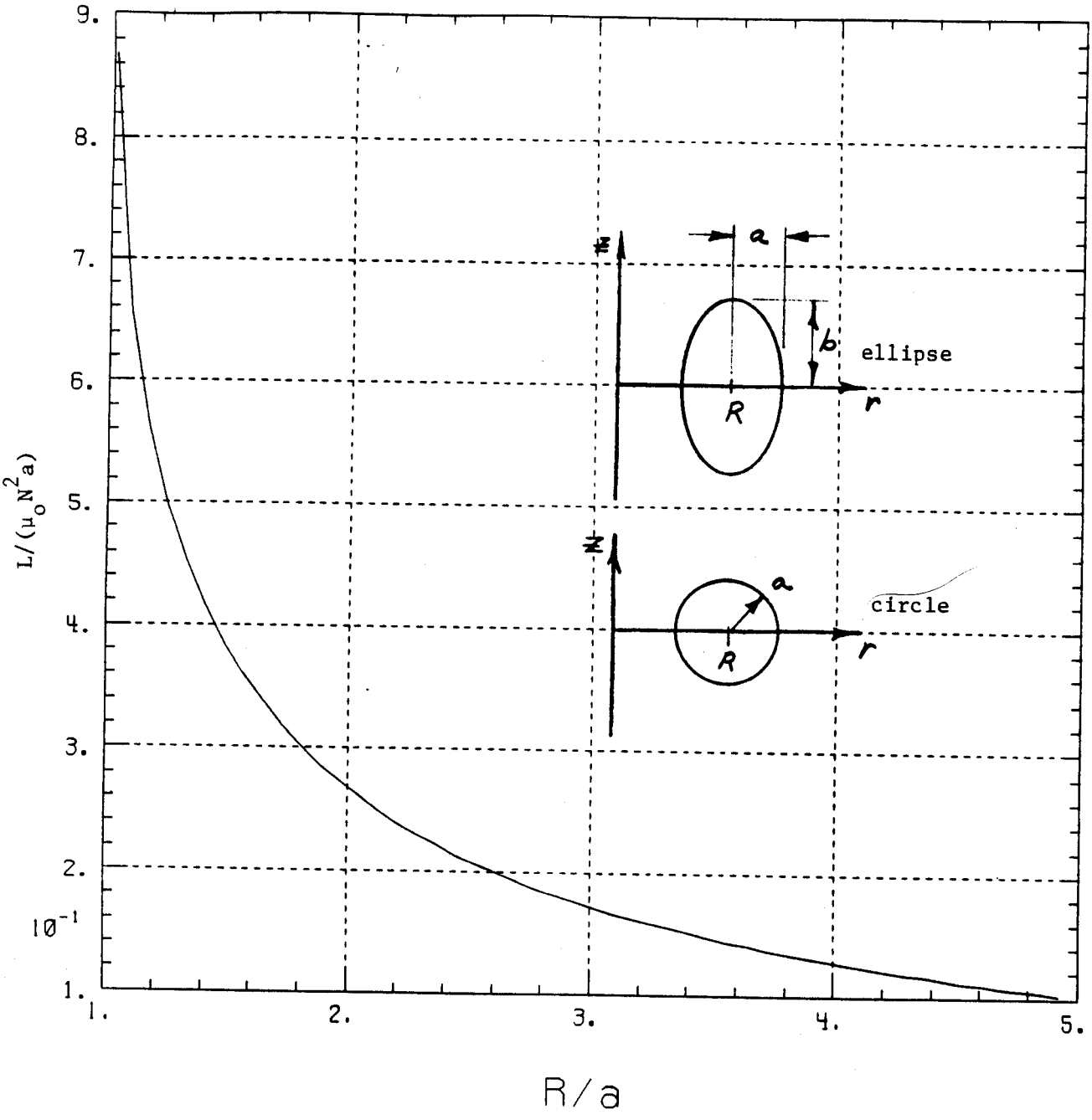

Fig. 4.1 Normalized Inductance or Energy For a Thin Torus With Circular or Elliptical Cross-Section

$$k = \frac{4\pi T}{\mu_0 (NI)^2} \tag{4.2}$$

where T = tension in torus half and NI = total ampere turns in the torus.

The inner and outer extreme radii are related to the tension parameter by:

$$k = \frac{1}{2} ln(r_2/r_1) \tag{4.3}$$

The inductance is then given by [4]:

$$\frac{L}{\mu_0 r_0 N^2} = \frac{1}{2} k^2 [I_0(k) + 2I_1(k) + I_2(k)] \tag{4.4}$$

where:

$$r_0 = \sqrt{r_2 r_1}$$

and

$$I_n(k) = \text{modified Bessel function of order n.}$$

The dimensions for the rectangular cross-section case are defined in Figure 4.3 which is also a plot of the normalized inductance. The expression for the latter is as follows:

$$\frac{L}{\mu_0 b N^2} = \frac{1}{\pi} \ln (r_2/r_1) \tag{4.5}$$

The formulae and plots in this section were obtained to allow easy estimation of the magnetic energy stored in toroidal field coil systems of selected cross-sectional geome-

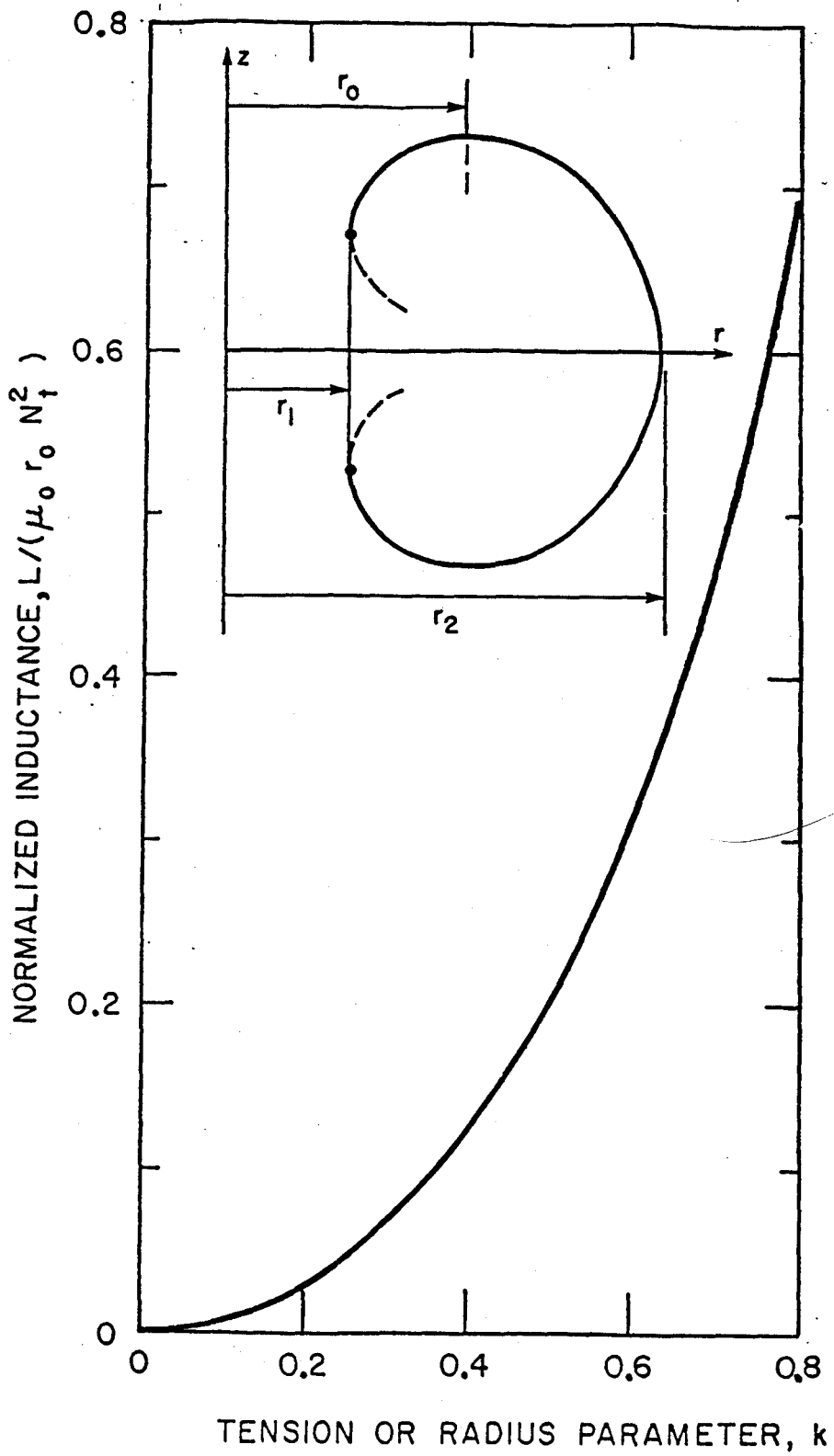

Fig. 4.2 Normalized Inductance or Energy For a Thin Torus With a "Princeton-D" Cross-Section

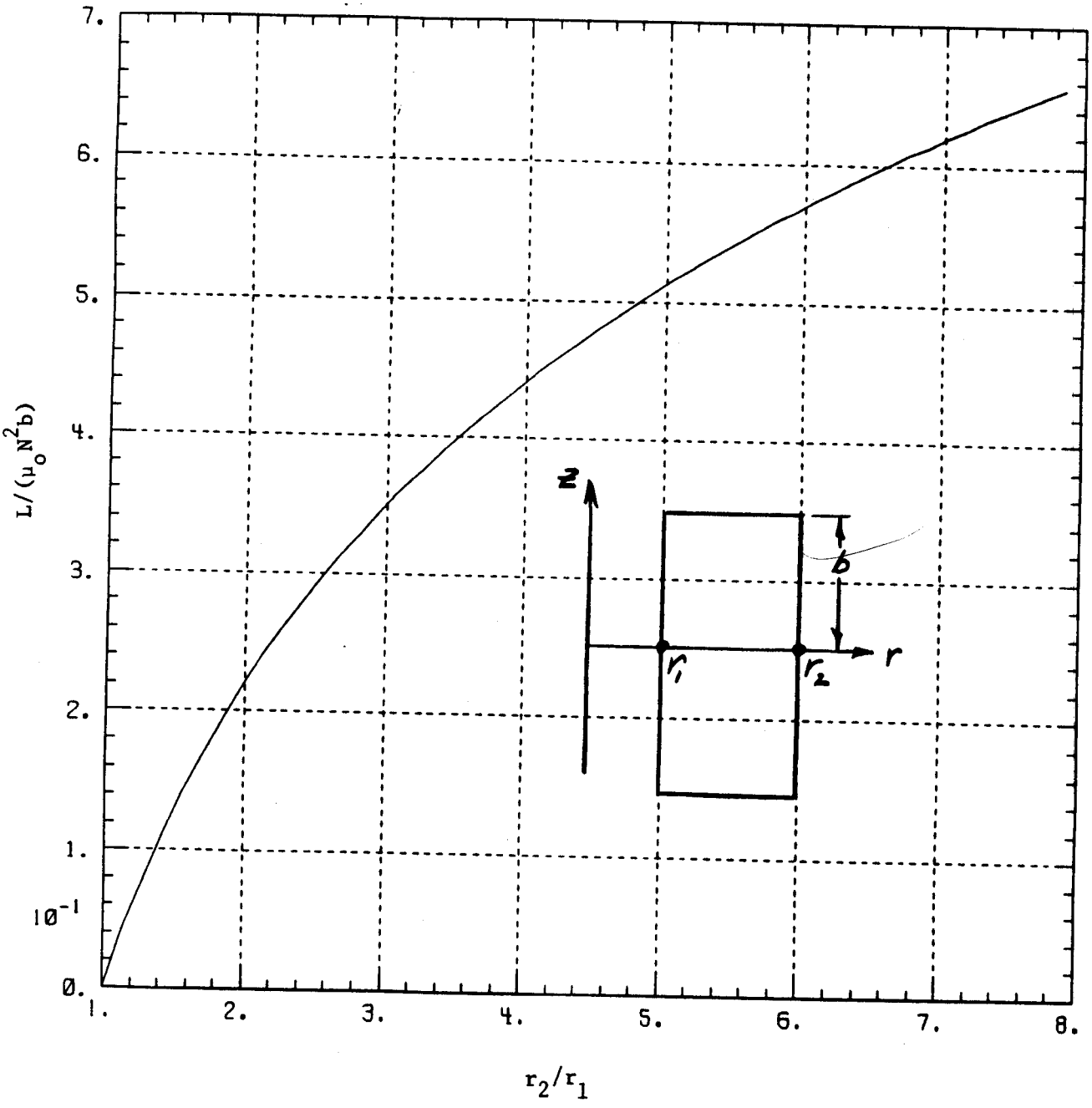

Fig. 4.3 Normalized Inductance or Energy For a Thin Torus With a Rectangular Cross Section

tries. They assume a thin shell type winding and will, therefore, underestimate the actual situation. However, they may be expected to be adequate for initial calculations.

——— References for Section 4.0

[1] R.J. Thome, R.D. Pillsbury, J.V. Minervini, et al, "Safety and Protection for Large Scale Superconducting Magnets - FY 1984 Report," PFC/RR-84-17, Section 2.0, Nov. 1984

[2] R.J. Thome, R.D. Pillsbury, W.G. Langton, and W.R. Mann, "Magnetic to Kinetic Energy Conversion Following Structural Failure," IEEE Trans on Magnetics, vol MAG-21, no 2, March, 1985.

[3] R.J. Thome and J.M. Tarrh, **MHD and Fusion Magnets: Field and Force Design Concepts**, Wiley, New York, 1982.

[4] S.L. Gralnick and F.H. Tenney, "Analytic Solution of the Toroidal Constant Tension Solenoid," 6th Symp on Engr Probs of Fusion Research, San Diego, 1975.

5.0 PULSE COIL FAILURE ANALYSIS

This section describes the unexpected failure of two pulse coil sets which were part of experiments designed to measure stability parameters of superconducting sample wire. The failures occurred during separate experimental runs with different test sample configurations within the pulse coil sets. An analysis is presented which attributes the pulse coil damage to two different failure modes.

5.1 Pulse Coil Description

Several pulse coil sets were constructed for an experimental program to study the stability of internally cooled cabled superconductors (ICCS) to electromagnetically coupled energy disturbances. The coaxial coil pairs were designed to provide magnetic pulses of several hundred tesla per second in an annular region which contained the sample ICCS. The pulse coils and sample were in a dc background field that ranged from 8 to 12 tesla, provided by a Bitter magnet.

A schematic of the pulse coil assembly is shown in Fig. 5.1. The photograph in Fig. 5.2 shows an empty pulse coil set without the top flange and axial tie rods. The coils were designed to have approximately equal NA (Turns $\times$ Area) and connected in series opposition in order to provide a fairly uniform pulse field at the sample while not coupling to the background field coil or conductive dewar shells. The pulse coil characteristics are summarized in Table 5.1. The coils were wound with copper magnet wire on phenolic bobbins. The coil ends were contained by phenolic flanges which were epoxied to the bobbins before winding. The wires were coated with heavy Formvar insulation. Both coils were overwrapped with several layers of epoxy-coated fiberglass tape.

Two separate but related experiments were done with different sample configurations

Table 5.1 Pulse Coil Characteristics

INNER PULSE COIL	
Inner Diameter	5.91 cm
Outer Diameter	7.81 cm
Height	12.7 cm
Number of Layers	5
Number of Turns	330
Self-Inductance	3.05 mH
Resistance (RT)	0.7 Ω
Conductor	# 14 Cu Magnet Wire
OUTER PULSE COIL	
Inner Diameter	11.43 cm
Outer Diameter	12.7 cm
Height	12.7 cm
Number of Layers	2
Number of Turns	106
Self-Inductance	0.902mH
Resistance (RT)	0.2 Ω
Conductor	# 12 Cu Magnet Wire
COMBINED PARAMETERS	
Mutual Inductance	0.85 mH
Total Inductance	2.25 mH
Total Resistance (RT)	0.9 Ω
(4.2 K)	1.1 mΩ
B/I	12 Gauss/Amp

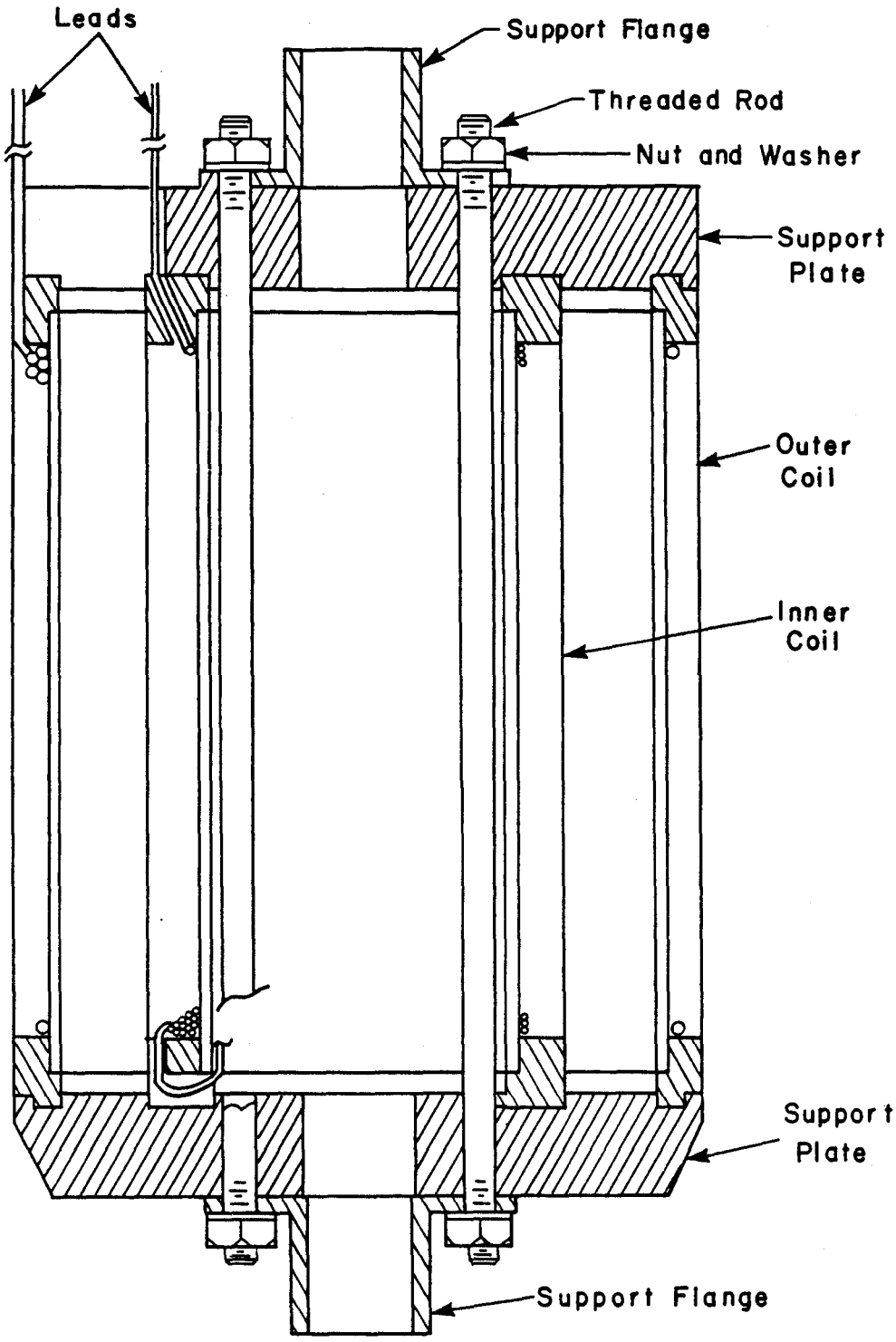

Fig. 5.1 Schematic of Pulse Coil Assembly

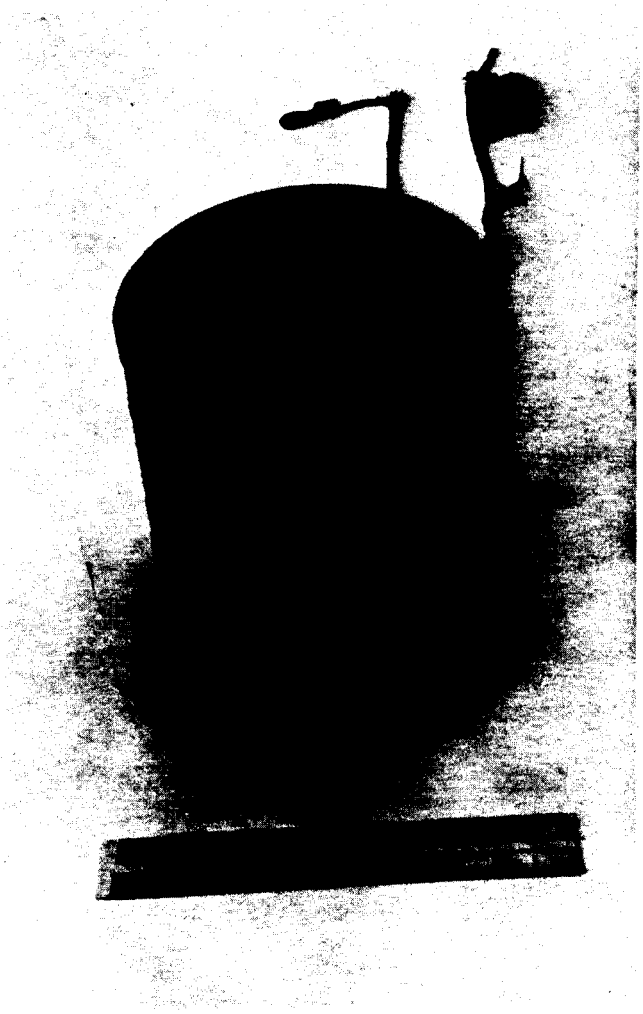

Fig. 5.2 Pulse Coil Set With Top Flange and Tie Rods Removed

in the pulse coil annulus. In the first configuration, the annular region was occupied by a sample coil that was wound with an ICCS, wrapped with fiberglass and potted in epoxy. This formed a rather rigid structure. There was approximately 0.050 inch radial clearance between the sample and the pulse coils. The second experimental configuration consisted of a vacuum chamber holding the sample conductor in the pulse coil annulus. The vacuum chamber was just a hollow 0.5 inch stainless steel tube which occupied approximately 310° at the pulse coil midplane. Thus, the annular region was mostly empty in this configuration.

5.2 Coil Operation

All tests were conducted with the pulse coil set and the sample immersed in liquid helium at 4.2 K and 1 atmosphere pressure. The pulse coils were suspended coaxial to the Bitter magnet with midplanes aligned. The dc field ranged from 0 to 12 tesla with the majority of pulses performed at the 10 tesla background field level.

The coils were pulsed by discharging a capacitor bank through them. The capacitor bank and control circuit were configured to give an underdamped sinusoidal pulse current at 50 Hz frequency which was interrupted after a half period. The pulse waveform could be selected to be either a single half-sinusoidal pulse of 10 ms duration or two half-sinusoidal pulses in succession, each of 10 ms duration (see Fig. 5.3). The coils were energized so that the field created by the pulse coils always subtracted from the background dc field in the annulus. This also caused the Lorentz force loads on the pulse coil set to always be in the same direction throughout the pulse cycle. Thus the net radial Lorentz forces on the outer pulse coil were always directed inward while the net Lorentz forces on the inner coil were always radially directed outward.

5.3 Failure Analysis

There were two independent failures of two separate pulse coil sets during different

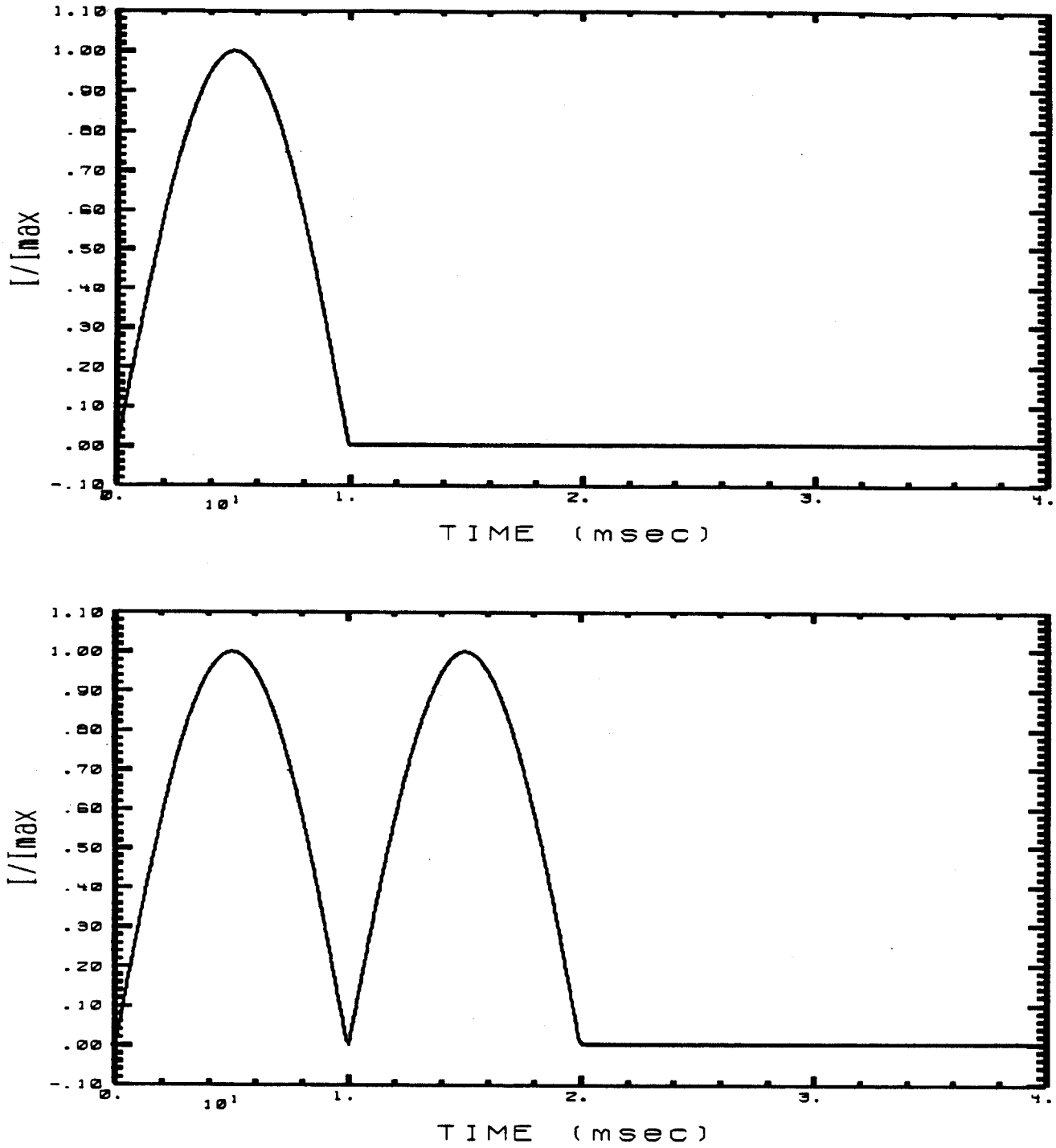

Fig. 5.3 Pulse Current Wave Form For a) Single Pulse, And b) Double Pulse

experiments. The first failure affected the inner pulse coil during an experiment in which the annulus was occupied by a potted sample coil. The failure consisted of the outer fiberglass wrap breaking under hoop tension and delamination of all the layers and turns of the inner coil. The structural failure allowed excessive radial movement of the turns which caused cracking of the Formvar insulation on the wires. Thus, some turn-to-turn and layer-to-layer arcing occurred. Figure 5.4 shows two views of the outer fiberglass wrap of the inner coil after the failure. The delaminated turns were removed. The dark areas evident on the inside of the wrap are pieces of Formvar insulation.

At the instant of the failure the operating conditions were capacitor discharged from 1750 volts, a maximum pulse coil current of 2475 amperes, and a background field of 10.2 tesla. The peak axial field at the inner pulse coil inner radius was 15.7 tesla. The coil failed during the most severe pulse of its life. It experienced approximately 134 pulses, the majority of which were in background fields of at least 8 tesla. In addition the coils had been thermally cycled from 300 K to 4.2 K and back approximately 8 times.

A simple analysis indicated an average internal pressure on the inner coil of 13,500 psi. Assuming the coil to be approximately 90% solid the hoop stress would be 54,000 psi which is greater than the yield strength of most coppers but close to the yield of CDA 102 drawn copper wire. If we use this as the yield strength than the strain at yield would be .0054 inch. The hoop stress in the fiberglass overwrap, under these conditions, would be only 19,000 psi. Calculations indicate that the fiberglass would carry an insignificant portion of the load. However, for the fiberglass to break, the copper would have had to creep and the strain would have been 0.0143 inch. The corresponding radial growth of the coil was 0.022 inch.

An estimate of the strain rate gave 0.0286/second. Thus creep may have been the cause of failure if the average stress in the copper was greater than the yield strength but

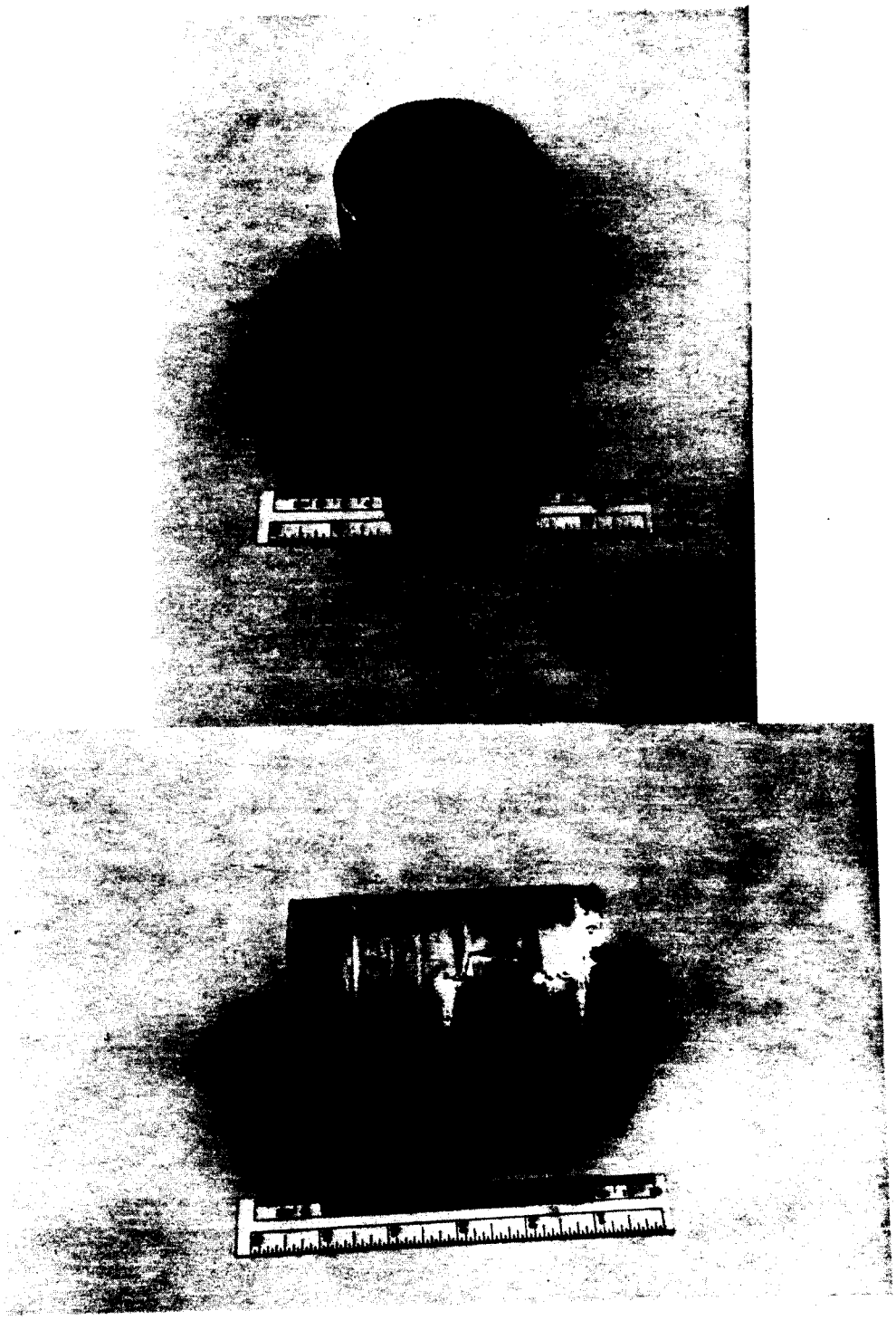

Fig. 5.4 Two Views of Inner Pulse Coil Fiberglass Wrap After Failure. Delaminated Copper Turns and Coil Mandrel Were Removed. Dark Areas on Inside of Fiberglass Wrap a) Are Remnants of Formvar Wire Insulation.

less than the ultimate strength. Unfortunately, the operating characteristics of these pulse coils calls for performance in this stress range. This leads to the conclusion that these coils will eventually fail due to creep unless the structure could be augmented or the coils redesigned.

The second pulse coil failure occurred under completely different circumstances. This failure of the outer pulse coil happened during an experiment in which the pulse coil annulus contained only the vacuum chamber and sample conductor within the chamber. The pulse history for this set was significantly less severe than for the previous experiment. In this case the background field was 10 tesla but the number and magnitude of the pulses were quite small. The pulse current at the time of failure was only 692 amperes.

The failure was obviously due to buckling of the outer pulse coil under hoop compression as can be seen in Fig. 5.5. The turns of the coil did not buckle like a complete ring because they were supported around most of their circumference (310°) by the vacuum chamber. A stress analysis of the coil, assuming each turn acted independently, gave an approximate compressive loading in the copper of 16,000 psi. This was very close to the critical buckling stress computed using an unsupported arch length of approximately 2 inches. If the coil had been fully potted so that the coil turns were bonded the critical stress would have been about 90,000 psi which is much greater than the loading.

Thus the solution to this problem was to just fill the annulus with a solid filler material that would carry some of the compressive load to prevent buckling. This is exactly the condition for the experiment with the potted sample coil in the annulus, and thus, it experienced much greater Lorentz force loadings without buckling.

5.4 Conclusions

Two sets of pulse coils failed in different modes under different operating conditions.

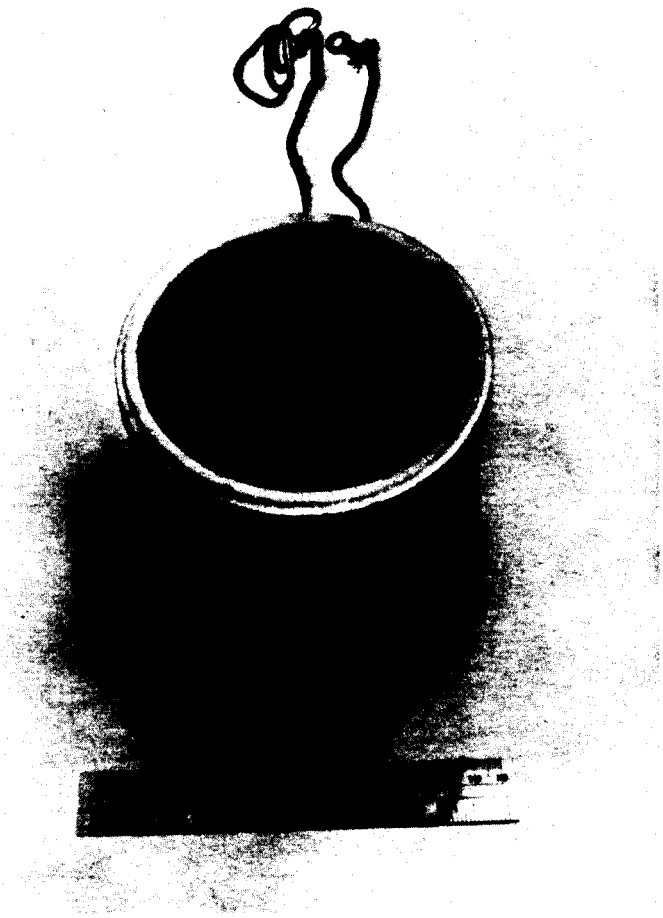

Fig. 5.5 Photograph of Outer Pulse Coil Which Failed Due to Bucking. Copper Turns Buckled Over About 50^o Arc Because the Remainder of the Circumference Was Partially Supported.

The first failure mode occurred due to creep in the copper turns of the inner pulse coil. The second failure occurred due to buckling of insufficiently supported thin rings (individual copper turns). In both situations the coils were being operated in a manner for which they were not initially designed. The solution to both problems is to redesign the coils by fully epoxy impregnating the windings, using a thicker walled or stronger material mandrel for the outer pulse coil and by using a thicker fiberglass overwrap on the inner pulse coil or distributing the fiberglass between the layers.

6.0 Safety Related Activities

6.1 GE/LCP Coil Short Circuit Analysis

In 1983, MIT provided computational support to ORNL in their successful attempt to burn out an instrumentation lead short circuit in the GE/LCP coil [1]. This past year, another short circuit was detected and MIT provided analyses to ORNL as part of this program. As of this writing, they plan to attempt a burn-out at a convenient point in the facility schedule. The following outlines the model and results of the burnout analysis performed this year.

Figure 6.1 shows the model which contains a single short in the coil which is driven at the terminals by an AC voltage source. The coil case is included as a collection of of six passive, short-circuited secondaries. The values used for this analysis are given in the following table.

TABLE 6.1

LUMPED PARAMETER CIRCUIT VALUES FOR GE LCP SHORT CIRCUIT ANALYSIS

L1 = 2.06 H.	R1 = 0.5457 ohm
Ls = 4.85e-3	Rs = 0.0219
L2 = 5.13e-6	R2 = 5.21e-4
L3 = 7.61e-6	R3 = 6.96e-4
L4 = 7.07e-6	R4 = 1.11e-3
L5 = 8.67e-6	R5 = 1.30e-3
L6 = 7.07e-6	R6 = 1.11e-3
L7 = 8.67e-6	R7 = 1.30e-3

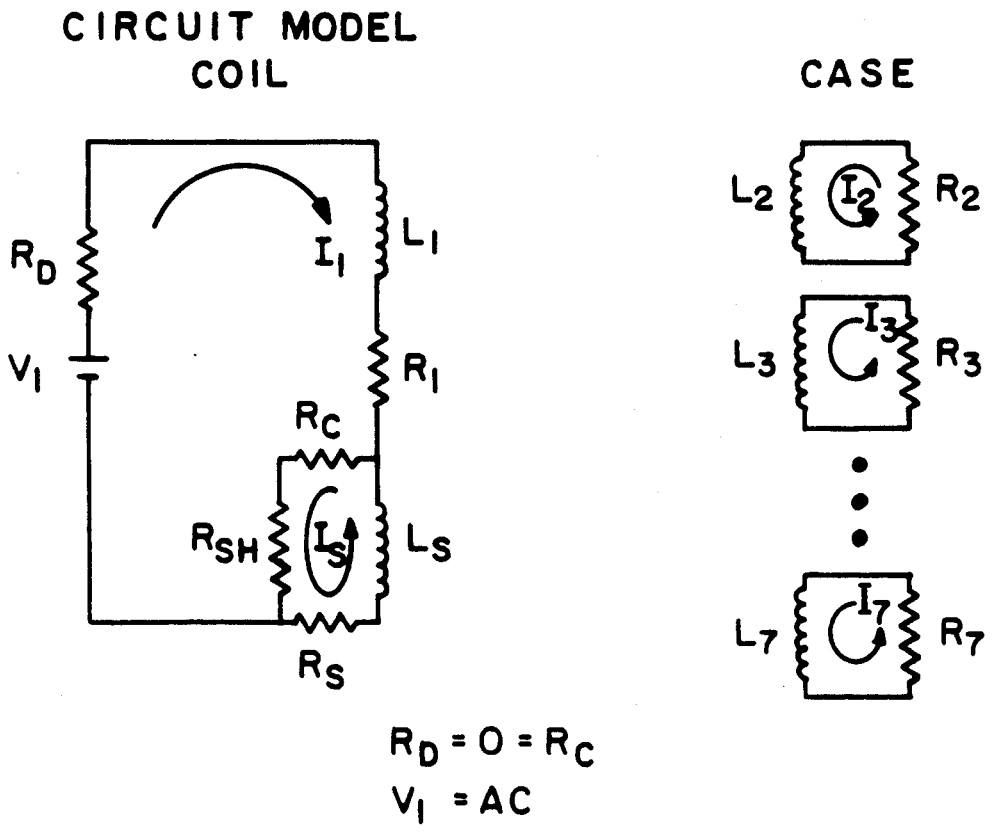

Fig. 6.1 Circuit Model for GE/LCP Short

R_{sh} was taken as 0.66 ohm at room temperature and varied with temperature. Coil section dimensions and short location in this study are summarized in Fig 6.2 and Table 6.2. Based on ORNL data it was assumed that the short ran from a point between the 3rd and 4th pies out of a total of 12 pies, that the short was across the inner 25 turns out of 54 in pie number 4, and that the short was a 28 gauge instrumentation wire. The entire coil was assumed to have a total of 648 turns and to be a solenoid for simplicity. Resistances and inductances were calculated for the individual coil sections, then the values were collapsed into an equivalent circuit.

TABLE 6.2

CHARACTERISTICS OF REGIONS IN FIGURE 6.2

region n	turns in region	R_n (Ω)	r_1 (cm)	r_2 (cm)	z_1 (cm)	z_2 (cm)
A	162	0.1419	165	212	- 26.3	- 13.2
B	29	0.0254	187	212	- 13.2	- 8.77
C	25	0.0219	165	187	- 13.2	- 8.77
D	432	0.3784	165	212	- 8.77	26.3

Figure 6.3 shows the computed temperature of the short as a function of time for selected coil terminal voltages. Both peak amplitude and rms values for the latter are given in the figure. In these estimates, the temperature rise is adiabatic and the temperature effect on the resistivity of the shorting wire is included. There may be considerable uncertainty in the property correlations at high temperatures. We have shown 1200 K as the burnout temperature. Figure 6.4 shows the rapid decay in current through the short with time because of its temperature rise.

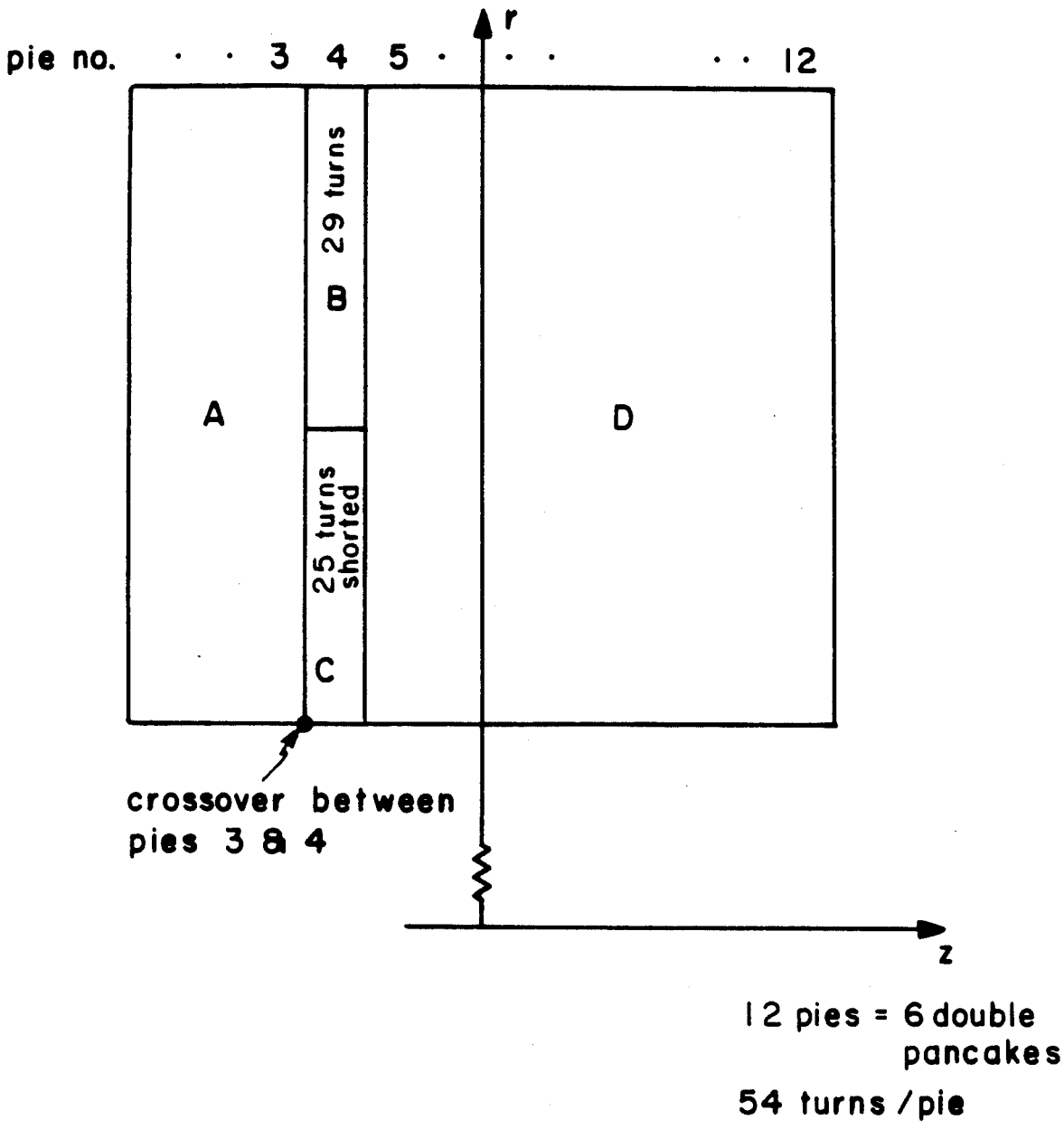

Fig. 6.2 GE/LCP Coil Cross Section Model

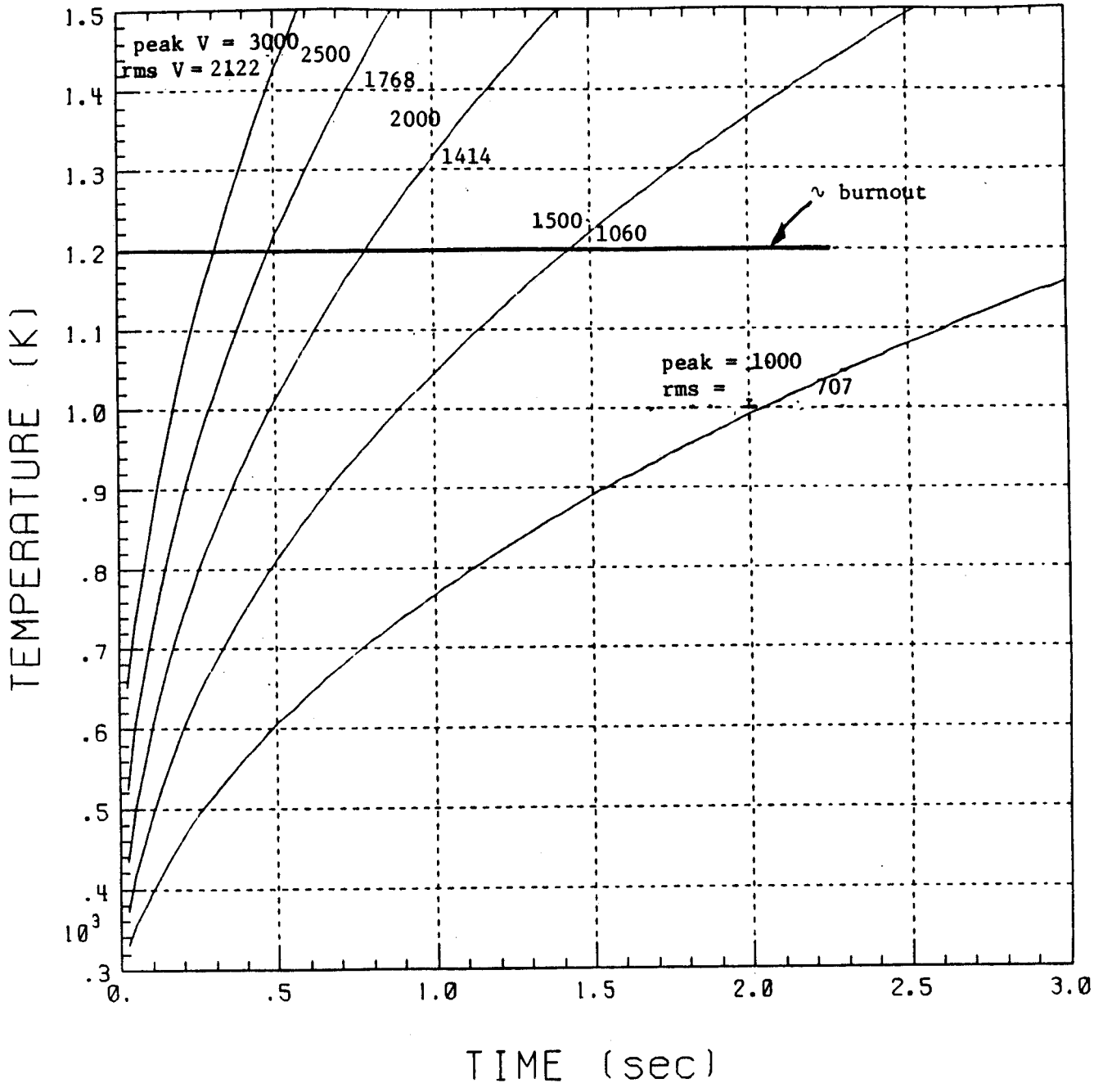

Fig. 6.3 Temperature of Short Assuming Adiabatic Conditions and a 28 Gauge Wire

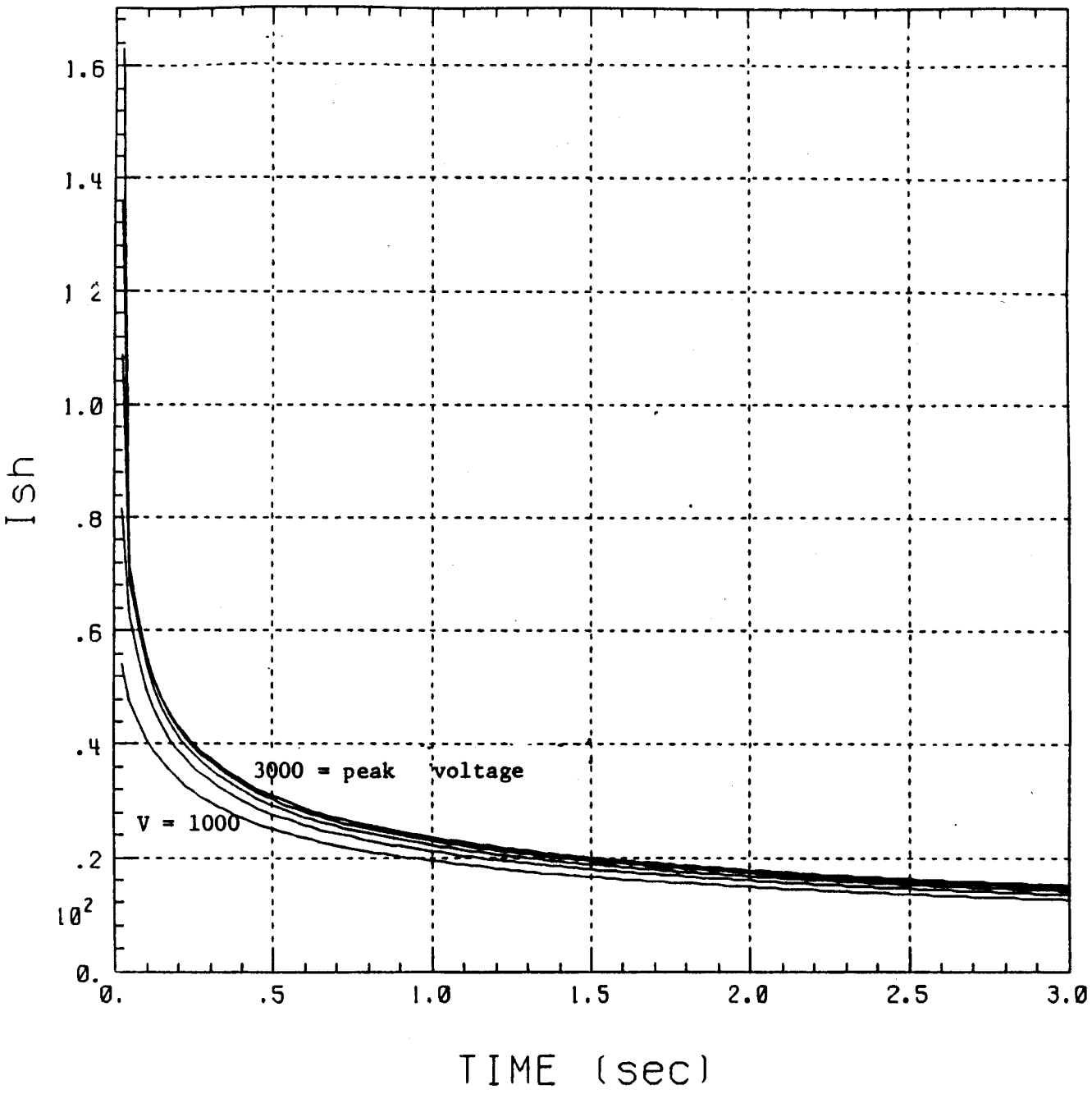

Fig. 6.4 Current (Peak AC) Through Short Vs. Time For Selected Coil Terminal Voltages

The thermal diffusion time constant for the wire insulation was estimated to be between 90 and 500 ms for thicknesses of 0.004 and 0.010 in., respectively. This implies that the adiabatic assumption in the model will only be valid on a time scale faster than this. It also implies that the ability to burn out the short with a minimum of melted insulation and charring in the vicinity of the instrumentation wire is dependent on depositing the energy in the wire on a time scale faster than this. Figure 6.3 shows that a temperature rise in burnout on a time scale faster than 0.5 s requires voltages higher than 1800 V_{rms}. From this standpoint, the higher the better since it is unlikely that the insulation is as thick as 0.010 in. and the use of low voltages will only "fry" things with a low probability of short removal. Since AC testing is probably not as severe as DC, it should be possible to apply a peak AC voltage at least as high as the DC high-pot voltage used for QC in fabrication. This area requires review by ORNL in the process of choosing a voltage.

It is our opinion that the likelihood of making and breaking other shorts in this coil during operation is quite high. Estimates should be made of effects within the coil, in the quench detection system, and potential interactions between coils during operation in the event that a short makes or breaks during charge or discharge.

6.2 Grad Course Case Study

In FY1984 we completed our study [2] of the structural failure of a large MHD magnet which occurred in Dec. 1982. This past year, T.M. Mower, a grad student at the PFC, used the results as the basis for an extensive report in Advanced Engineering Mechanics (CE 1.132) [3]. The goal of the course is to develop a series of case studies written for sophomore engineers to illustrate potential problem areas in design. Passing this type of information on to engineering students is important since our own studies have shown that a primary factor contributing to failure incidents is design error (see Section 3.0).

———— References for Section 6

[1] J.F. Ellis, M.S. Lubell, S.S. Shen, P.L. Walstrom, R.J. Thome, & R.D. Pillsbury, "Shorts Due to Diagnostic Leads," Proc of the 1984 Applied Superconductivity Conference, San Diego, September,1984.

[2] R.J. Thome, R.D. Pillsbury, J.V. Minervini, et al, "Safety and Protection for Large Scale Superconducting Magnets-FY1984 Report," PFC/RR-84-17, Nov, 1984.

[3] T.M. Mower, "Incident at the Magnetohydrodynamic (MHD) High Performance Demonstration Experiment (HPDE)," submitted to MIT in partial fulfillment of the requirements for CE 1.132, May 14, 1985.